Low-velocity thermonuclear curved detonations in Type-Ia supernovae with a detailed nuclear network*

Abdelmalek El Messoudi[a], Pierre Vidal[b], Yves Busegnies[a]

[a]Institut d'Astronomie, Université Libre de Bruxelles, Campus Plaine, CP 226, 1050 Bruxelles, Belgique

[b]Laboratoire de Combustion et de Détonique, UPR 9028 CNRS, ENSMA, BP 40109, 86961 Futuroscope, France

1 Introduction

A Type-Ia supernova (SNIa) is now described as the result of the thermonuclear explosion of a compact and dense Carbon-Oxygen star called "white dwarf". However, the ignition stage and the propagation mode of the combustion wave are not identified yet. Thus, the considered mechanisms are a pure deflagration or a deflagration-to-detonation transition process [13],[8]. In terrestrial explosives, the dynamical detonation behaviours result from a very strong hydrodynamics-chemical kinetics interplay. For example, in homogeneous gases, these are the cellular structures characterizing the intrinsic local instability of the reaction zone or the very sudden extinctions and transverse reignitions observed in the limiting initiation by point-source energy release or in the transmission from a tube to a large volume. These behaviours are determined by the number and the relative importance of the energy-release steps : the head of the release wave - the "sonic surface" - that partly or fully limits the reaction zone of the self-sustained detonation can thus be located at the end of the last step or of an intermediate one, depending on whether the flow divergence is weak or strong. The former case defines CJ (Chapman-Jouguet) or quasi-CJ regimes and the latter defines the so-called low-velocity detonation regimes, because only a limited amount of the available energy sustains the shock. As a rule, each step is associated with a cell size and an existence condition such as the ignition energy, the transmission diameter or the detonation radius. Indeed, the characteristic lengths of these phenomena are strongly correlated to that of the energy-release process in one-dimensional steady detonation. The simulations can represent these dynamics only if all cellular levels are simultaneously accounted for because, for example, a local re-ignition results from the unsteady, three-dimensional flow prior to extinction [15],[14],[9],[10]. To our knowledge, such simulations have not been performed yet in the astrophysical context. Since no spontaneous ignition mechanism (e.g., TDD or point-source explosion) is able to generate a planar flow, we here study existence conditions for the self-sustained (sonic) detonation regime in Type-Ia supernovae by means of a curved detonation model. We consider a weakly-curved detonation that propagates with a speed D that increases to the planar value limit when its curvature κ decreases if the latter is smaller than a maximum (critical) value. Often discussed for gaseous terrestrial detonations [11],[19], this model provides a good average of the behavior of a curved cellular detonation before relaxation to the planar regime because experiments show that cell sizes are small compared to the curvature radius. If energy is released in one step, the $D(\kappa)$ relationship shows a unique critical point -defining the smallest detonation radius and velocity- that results from the use of a rate law sufficiently sensitive to temperature (e.g. the Arrhenius law and its nonlinearity produced by a large activation energy). We only present results for the 50% C - 50% O plasma with initial temperature and density $T_0 = 2 \times 10^8$ K and $\rho_0 = 5 \times 10^6$ g.cm^{-3}. Our calculations are made with a very detailed kinetic network comprising 331 nuclids linked

*A 6-pages abstract submitted with kind permission of Professor Nikita Fomin

Correspondence to : pierre.vidal@lcd.ensma.fr

by 3262 capture or photodisintegration reactions that includes strong and electromagnetic interaction processes [6]. First, we study the energy release process for the planar steady detonation. This model detonation is the exact representation of the average behavior of the actual cellular detonation far from its propagation limits and its study is the primary step for characterizing the energy release process. We confirm the 3 fundamental decomposition steps of this mixture - the successive combustions of ^{12}C, ^{16}O and ^{28}Si - before asymptotic relaxation to nuclear statistical equilibrium, [12],[1], but we show that theirs lengths can be 200 times smaller than those usually obtained with reduced networks. Next, we study the conditions for propagation of curved detonations. We show that, in this plasma, the flow divergence yields two low-velocity regimes and conditions for propagation - associated, respectively, with 80% and 40% only of the theoretically available energy -, significantly increases the lengths of the energy-release steps, even suppressing the longest ones, thereby leading to an incomplete nucleosynthesis very different from that resulting from the planar detonation regime.

2 Reaction zone and evolution of curved detonations

Our analysis is restricted to planar ($j = 0$), cylindrically- or spherically-symmetric ($j = 1$ ou 2) self-sustained detonations. The dependency domain can be considered as steady under the assumption, to be checked after the fact (Tab.2), that its thickness ℓ_S is always much smaller than the shock radius R, i.e. $\varepsilon = \ell_S/R \ll 1$. The balance and kinetics equations then reduce to

$$(D-u)\frac{d\rho}{d\xi} - \rho\frac{du}{d\xi} + j\frac{\rho u}{R-\xi} = 0, \quad \rho(D-u)\frac{du}{d\xi} - \frac{dp}{d\xi} = 0, \quad \frac{de}{d\xi} - \frac{p}{\rho^2}\frac{du}{d\xi} = 0, \quad \frac{d\mathbf{Y}}{d\xi} = \frac{\mathbf{w}}{D-u}. \qquad (1)$$

ξ is the distance from the shock ($\xi \leqslant \ell_S \ll R$), ρ, u, p and e denote the density, the material speed in the Laboratory reference frame, the pressure and the specific internal energy. $\mathbf{w}(\rho, T, \mathbf{Y})$ is the vector of the reaction rates, T is the temperature and $\mathbf{Y}$ is the vector of the molar abundances Y_i (mole number per unit mass, $i = 1, .., N$). System (1) is closed with the two functionals $p = p(\rho, T, \mathbf{Y})$ and $e = E(\rho, T, \mathbf{Y}) + Q(\mathbf{Y})$ of the equation of state, which, very classically for the considered mixture, represent a gas of particles without interaction with Maxwell-Boltzman distributions for the ions, an arbitrarily-degenerated and relativistic Fermi-Dirac distribution for the electron-positon pairs and a Bose-Einstein distribution for the photons in equibrium with matter [18]. $Q = N_a \sum_i Y_i B_i$ is the total binding energy with N_a, N and B_i the Avogadro number, the nucleid number, and the binding energy (< 0) of nucleid i. In the planar case ($j = 0$), the 3 balances (1a-c) can be integrated for any $\xi \geqslant 0$ and any $\mathbf{Y}$, and written under the Rankine-Hugoniot (RH) form,

$$\rho\,(D-u) = \rho_0 D, \qquad p + \rho\,(D-u)^2 = p_0 + \rho_0 D^2, \qquad e + \frac{p}{\rho} + \frac{(D-u)^2}{2} = e_0 + \frac{p_0}{\rho_0} + \frac{D^2}{2}, \qquad (2)$$

where D is the detonation velocity and the index 0 denotes the pre-shock state. These relations also connect the pre- and post-shock states ($\xi = 0$) whatever the geometry ($j \geqslant 0$). Denoting by $\kappa = j/R$ the shock total curvature, the assumption $\varepsilon \ll 1$ gives the approximation $j/(R-\xi) = \kappa\,(1 + O\,(\varepsilon))$ and system (1) can be written as an ordinary system of differential equations

$$\frac{d\rho}{d\xi} = \frac{-\rho}{(D-u)}\,\frac{\boldsymbol{\sigma}.\mathbf{w} - uM^2\kappa}{1-M^2}, \quad \frac{dp}{d\xi} = -\rho(D-u)\,\frac{\boldsymbol{\sigma}.\mathbf{w} - u\kappa}{1-M^2}, \quad \frac{du}{d\xi} = \rho(D-u)\frac{dp}{d\xi}, \qquad (3)$$

$$\frac{dT}{d\xi} = \left.\frac{\partial p}{\partial T}\right|_{\rho,\mathbf{Y}}^{-1} \left((D-u)^2 - \left.\frac{\partial p}{\partial Y}\right|_{\rho,T}\right)\frac{d\rho}{d\xi} - \sum_i \left(w_i \left.\frac{\partial p}{\partial Y_i}\right|_{T,\rho,Y_{j\neq i}}\right) - \rho u\,(D-u)^2\,\kappa, \quad \frac{d\mathbf{Y}}{d\xi} = \frac{\mathbf{w}}{D-u}.$$

$\boldsymbol{\sigma}.\mathbf{w}$, a_f et $M = (D-u)/a_f$ denote the thermicity, the frozen sound speed and the flow Mach Number in the shock frame. Given a pre-shock state and a celerity value D, the RH equations (2) and the equation of state define the initial conditions at $\xi = 0$ for integrating (3) towards the reaction-zone end. For a sonic detonation, there exists a value of the curvature κ for each value of D such that the sonicity ($D = u + a_f$ or $M = 1$) and thermicity ($\boldsymbol{\sigma}.\mathbf{w} - u\kappa = 0$) constraints are simultaneously fullfilled at some moment of the integration (i.e. $\xi > 0$) thereby discarding non-physical (infinite) derivatives. This detonation thus obeys an eigenvalue evolution law $D(\kappa)$ that can be numerically obtained by numerical shooting towards the saddle point ($M = 1$, $\boldsymbol{\sigma}.\mathbf{w} = u\kappa$). The flow divergence, here approximated by the curvature term, thus acts as an adiabatic process that counteracts the exo-energetic decomposition process. For the considered plasma and pre-shock conditions, the limit $\kappa \to 0$ gives the ("frozen") planar detonation velocity D^f_{CJ}, which can be calculated assuming the plasma at the nuclear statistic equilibrium (NSE) and is found here very-slightly larger than the equilibrium CJ value D_{CJ} (Table 1). A more detailed discussion of these classical issues is out of the scope of this paper [5],[12].

3 Discussion

We have carried out these calculations with a detailed nuclear network comprising 331 nucleids and 3262 capture and photodesintegration reactions that include the electromagnetic and strong-interactions processes [1], and with the reduced network comprising 13 nucleids and 27 reactions [13] used by Sharpe [16],[17]. The steady-reaction profiles for the planar detonation (Figure 1, left) for the detailed network confirm the 3 fundamental steps of the energy release previously identified [12], i.e. the successive combustions of C, O and Si asymptotically leading to the NSE. However, the combustion lengths of ^{16}O and ^{28}Si are 10 times shorter and the total reaction length is 20 times shorter than with the reduced network. The differences with the results obtained by Gamezo and al. [7] are even larger, their Si-combustion and NSE-relaxation lengths being respectively 100 and 200 longer than ours. We also observe significant differences in the abundances, depending on the considered network, and that the decomposition process for the detailed network, though the faster, starts with the smaller post-shock temperature and density (Table 1).

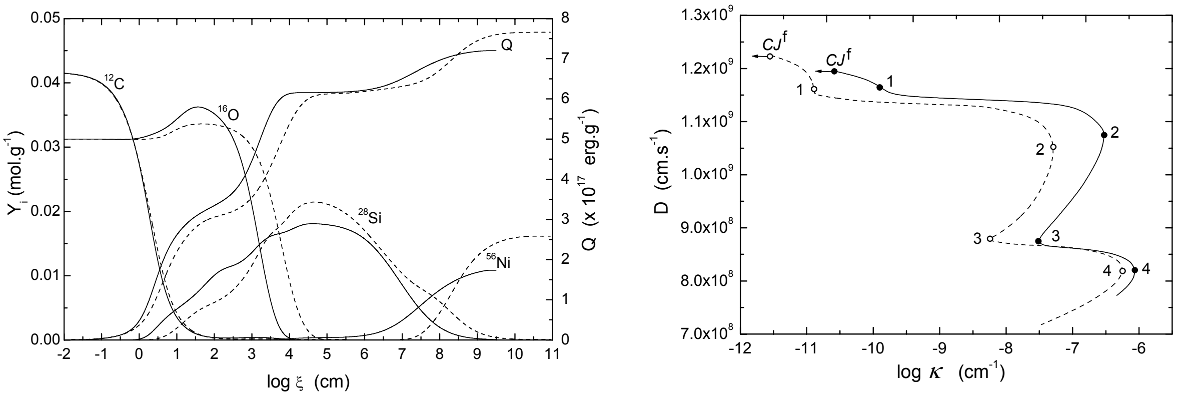

Figure 1. Left : abundance (Y_i) (left scale) and released energy (Q) (right scale) profiles for the planar steady sonic detonation. Right : Celerity (D) - Curvature ($\kappa = j/R$) relationship for curved steady sonic detonations. Solid lines : 331-nuclide detailed network. Dashed lines : 13-nuclide reduced network.

Whichever network is considered, the $D(\kappa)$ evolution law of curved detonation (Figure 1, right) shows 2 branches with negative slopes and 4 singular points, 3 being critical (infinite slopes). Given the radius (or the curvature), the velocities associated with the reduced network are the smaller. Indeed, the planar reaction lengths - the only reference lengths in the problem - are much smaller with the detailed network (Figure 1, left and Table 1) and it is easy to check that the gap between the $D(\kappa)$ curves is about in inverse proportion to the ratio of the lengths associated with each network. The upper branch is located between the CJ^{f} point and the first critical point (2) and the lower branch is located between the second and the third critical points (3 and 4). The reaction profiles (Figure 2) show that each branch corresponds to a distinct step of the energy release. More quantitatively, dimensional considerations imply that the relative differences in the velocities for each radius are about half those for the energies at the sonic surface ($D^2 \propto Q \Rightarrow 2\Delta D/D \approx \Delta Q/Q$), as is confirmed in Table 2. The detonations associated with the interval $CJ^{\mathrm{f}} - 1$ of the upper branch are quasi-CJ because their maximal deficit is always smaller than 5% and the 3 fundamental steps of the plasma decomposition are preserved. However, the decompositions of ^{12}C et ^{16}O about Point 1 are 10 times longer than in the planar case, and the ^{28}Si combustion and the ^{56}Ni production are incomplete. This lengthening results from the decrease in the reaction rates, which are all the smaller as the temperature (or the shock velocity) is smaller ($T \propto D^2$).

Number of nucleids	D_{CJ}	D^f_{CJ}	$\ell_{^{12}\mathrm{C}}$	$\ell_{^{16}\mathrm{O}}$	$\ell_{^{28}\mathrm{Si}}$	ℓ_*	T	ρ
331	1.187×10^9	1.207×10^9	10^2	10^4	10^9	5×10^9	4.09×10^9	2.28×10^7
13	1.199×10^9	1.237×10^9	10^2	10^5	10^{10}	10^{11}	4.21×10^9	2.31×10^7

Table 1. Equilibrium and frozen CJ detonation velocities ($cm.s^{-1}$) and C, O and Si combustion lengths (cm), total reaction length (ℓ_*, cm), post-shock temperature (T, K) and density (ρ, g.cm^{-3})

Number of nucleids	D^f_{CJ} Q_{CJ} R_{CJ} ℓ_*/R_{CJ}	D_1 Q_1 R_1 ℓ_{s1}/R_1	D_2 Q_2 R_2 ℓ_{s2}/R_2	D_3 Q_3 R_3 ℓ_{s3}/R_3	D_4 Q_4 R_4 ℓ_{s4}/R_4
331	1.207×10^9 7.170×10^{17} ∞ /	1.164×10^9 6.560×10^{17} 8.696×10^9 7×10^{-3}	1.074×10^9 5.850×10^{17} 6.623×10^6 1.8×10^{-2}	8.522×10^8 2.920×10^{17} 5.479×10^6 9×10^{-3}	8.208×10^8 2.860×10^{17} 2.296×10^6 1.4×10^{-2}
13	1.237×10^9 7.650×10^{17} ∞ /	1.162×10^9 7.000×10^{17} 1.657×10^{11} 1×10^{-2}	1.052×10^9 5.560×10^{17} 3.915×10^7 1.9×10^{-2}	8.655×10^8 2.980×10^{17} 4.081×10^7 2×10^{-2}	8.166×10^8 2.860×10^{17} 3.546×10^6 1.5×10^{-2}

Table 2. Planar- and curved- detonation velocities (D^f_{CJ} and D_i, $cm.s^{-1}$), released energies (Q_{CJ} and Q_i, erg/g), spherical curvature radius ($R_i = 2/\kappa$, cm) and ratios of the shock-to-sonic-locus distance (ℓ_{si}) to the curvature radius R_i at the singular points $i = 1, 2, 3, 4$ of the evolution law $D(\kappa)$ in Fig.1.

The network choice also induces important quantitative differences : the ^{28}Si residue is 60% or 20% and the ^{56}Ni production is 30% or 40% with the detailed or the reduced network. The inflexion at Point 1 represents a clue of a bifurcation to another branch with negative slope, for example for other initial conditions [2]. These differences are accentuated for the detonations in the interval $1 - 2$ of the upper branch. As the first critical point (Point 2) is approached, the maximal velocity deficit moves to 11% or 15% with the detailed or the reduced networks, the ^{28}Si combustion and the ^{56}Ni production disappear, the ^{16}O combustion is not complete, with 15% or 25% residues with the detailed or the reduced networks, and the decomposition lengths are further increased by a factor larger than 10. The detonations associated with the lower branch are characterized by velocity deficits of about 30%, the absence of ^{16}O and ^{28}Si decomposition, and, for the latter, abundances that only represent 20% of those at upper branch. Finally, even if the ^{28}Si production is considerably delayed, its maximum abundance occurs sooner than at the upper branch. The low-velocity regime associated with the upper branch $CJ^{\mathrm{f}} - 2$ was already observed by Sharpe [16] but to our knowledge, the one associated with the lower branch $3 - 4$, for which the detonation propagates with only 40% of the theoretically available energy, had not been identified yet. It is likely that Sharpe's calculations were not conducted for low-enough velocities.

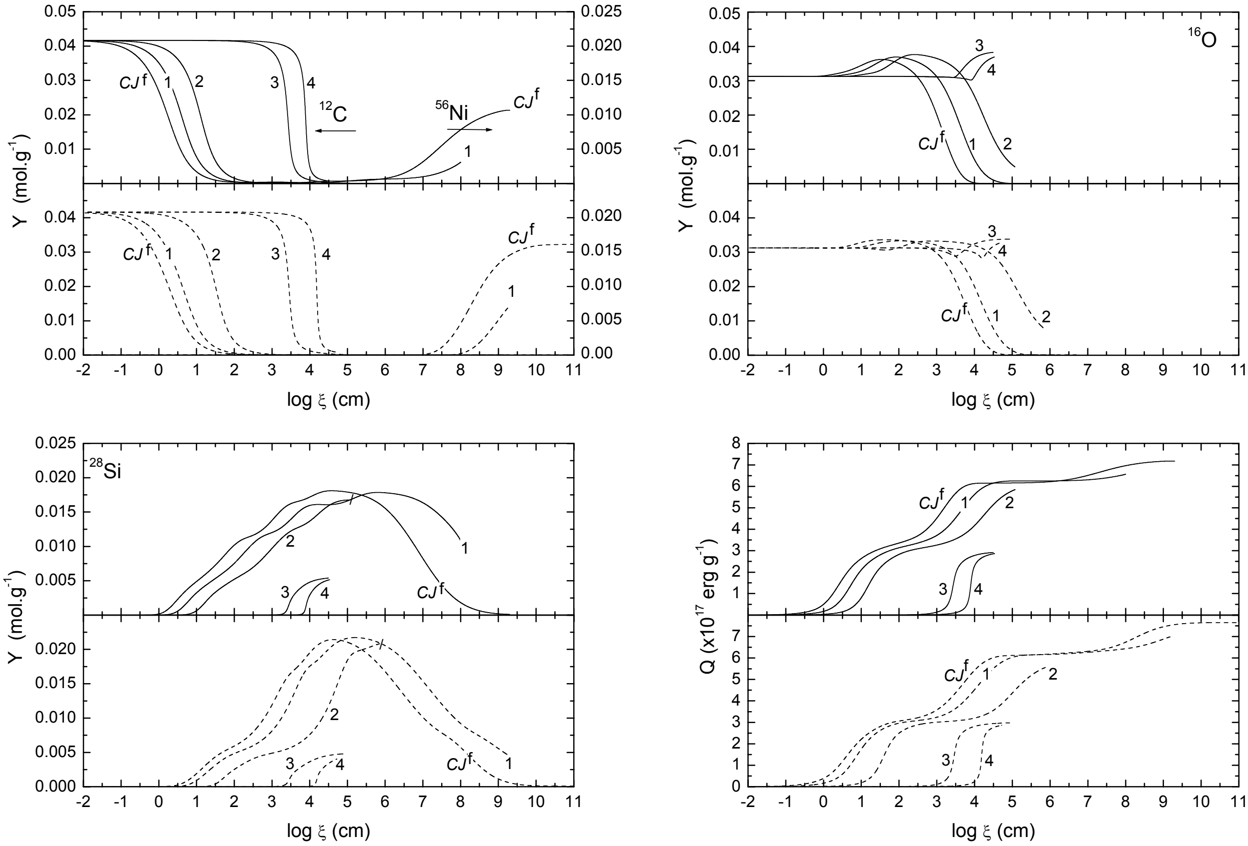

Figure 2. Abundance profiles (Y) for ^{12}C (left scale), ^{16}O, ^{28}Si, ^{56}Ni (right scale) and for the released energy (Q) for steady sonic detonations. Solid lines : 331-nuclide detailed network. Dashed lines : 13-nuclide reduced network. Planar case : $CJ^{\,\mathrm{f}}$. Curved cases : $i = 1, 2, 3, 4$, singular points of the evolution law $D(\kappa)$ in Fig.1. The symbol / shows the end of curve 2.

We thus show that in the 50% C - 50% O plasma at $T_0 = 2 \times 10^8$ K and $\rho_0 = 5 \times 10^6$ g.cm^{-3}, the flow divergence induces 2 low-velocity regimes and 2 conditions for curved detonation propagation, considerably increases the energy-release steps, and may even suppress the longest ones. As for the nucleosynthesis, and in the framework of spectrometric or photometric analysis of Type-Ia supernovae, we notice the very small production of ^{28}Si and of ^{56}Ni and the persistence of ^{16}O in the low-velocity regime. In terrestrial heterogeneous explosives, gaseous or condensed, the energy release results from an interplay between chemical kinetics and transport phenomena (hot-spots mechanisms, phase transfers) and may be accomplished in several steps. These physico-chemical descriptions have also produced $D\,(\kappa)$ curves with several critical points that quantitatevely account for experimentally-observed low-velocity detonation regimes in cylindrical tubes [3],[4]. In terrestrial homogeneous gases, the experiments show that the extinction and re-initiation phenomena are strongly unsteady, tridimensional and transverse to the mean flow direction. To date, the only realistic representations are numerical simulations that simultaneously solve all the levels of cellular structures [9],[10]. To our knowledge, this remains to be done in stellar plasmas.

References

[1] Aikawa M. , Arnould M., Goriely S., Jorissen A., Takahashi K. (2005). BRUSLIB and NETGEN: The Brussels nuclear reaction rate library and nuclear network generator for astrophysics, A&A, 441: 1195.

[2] El Messoudi A. (2008). Modélisation des détonations thermonucléaires en plasmas stellaires dégénérés : applications aux supernovae de type Ia. Thèse de l'Université Libre de Bruxelles.

[3] Ermolaev B.S., Khasainov B.A., Presles H.-N., Vidal P. (2005). A simple approach to reaction rate modelling in shocked multi-component solid explosives, European Combustion Meeting, Louvain-la-Neuve.

[4] Ermolaev B.S., Khasainov B.A., Presles H.-N., Vidal P., Sulimov A. (2005). Low-velocity detonation in ammonium nitrate and its mixtures, 13^{th} Symp. on Combustion and Explosion, Chernogolovka, Russie.

[5] Fickett W.C., Davis W. (1979). Detonation, University of California Press, Berkeley.

[6] Fryxell B.A., Müller E., Arnett D.A. (1989). Hydrodynamics and Nuclear Burning, Technical Report, Max-Planck-Institut für Physik und Astrophysik, Garching.

[7] Gamezo V.N., Wheeler J.C., Khokhlov A.M, Oran E.S. (1999). Multi-level structure of cellular detonation in Type-Ia supernovae, Ap. J., 512: 827.

[8] Gamezo V.N., Khokhlov A.M., Oran E.S. (2005). Three-dimensional delayed detonation model of Type-Ia supernovae, Ap. J., 623: 337.

[9] Guilly V., Khasainov B.A., Presles H.-N., Desbordes D. (2006). Simulation numérique des détonations à double structure cellulaire, C. R. Acad. Sci. (Mécanique), Paris, 334: 679.

[10] Guilly V. (2007). Etude de la diffraction de la détonation des mélanges C_2H_2/O_2 dilués par l'Argon. Thèse de l'Université de Poitiers.

[11] He L., Clavin P. (1994). On the direct initiation of gaseous detonations by an energy source, J. Fluid. Mech., 277: 227.

[12] Khokhlov A.M. (1989). The structure of steady detonation waves in Type-Ia supernovae, MNRAS, 239: 785.

[13] Khokhlov A.M., Oran E.S., Wheeler J.C. (1997). Deflagration-to Detonation Transition in thermonuclear supernovae, Ap. J., 478: 678.

[14] Luche J., Desbordes D., Presles H.-N. (2006). Détonations des mélanges H_2-NO_2/N_2O_4, C. R. Acad. Sci. (Mécanique), Paris, 334: 323.

[15] Presles H.-N., Desbordes D., Guirard M., Guerraud C. (1996). Gaseous nitromethane and nitromethane-oxygen mixtures : A new detonation structure, Shock Waves, 6: 111.

[16] Sharpe G.J. (1999). The structure of steady detonation waves in Type-Ia supernovae : Pathological detonations on C-O cores, MNRAS, 310: 1039.

[17] Sharpe G.J. (2001). The effect of curvature on detonation waves in Type-Ia supernovae, MNRAS, 322: 614.

[18] Weiss A., Hillebrandt W. , Thomas H.C., Ritter H. (1979), in "Cox and Giuli's Principles of Stellar Structure", Cambridge (UK), Princeton Publishing Associates Ltd (2004).

[19] Yao J., Stewart D.S., (1996). On the dynamics of multi-dimensional detonations, J. Fluid. Mech., 309: 225.